JOURNAL OF TISSUE ENGINEERING AND REGENERATIVE MEDICINE
J Tissue Eng Regen Med 2016.
Published online in Wiley Online Library (wileyonlinelibrary.com) **DOI:** 10.1002/term.2145

RESEARCH ARTICLE

Collagen type I–PLGA film as an efficient substratum for corneal endothelial cells regeneration

Eun Young Kim†, Nirmalya Tripathy†, Sun Ah Cho, Dongwon Lee and Gilson Khang*
Department of BIN Fusion Technology, Department of Polymer Nanoscience and Polymer BIN Research Centre, Chonbuk National University, 567 Baekje-daero, Deokjin-gu, Jeonju, 561-756, Republic of Korea

Abstract

Surface modulations of desired biological construct design for regenerative medical therapy is considered to be highly crucial for cell growth and the subsequent regeneration of biologically competent tissues. In this study, we fabricated stable, transparent, collagen type-I-coated PLGA films (Col I–PLGA) as a potential substratum for the regeneration of corneal endothelial cells. Morphological and structural properties were analysed by FE–SEM, AFM, FTIR, contact angle, etc., and *in vitro* biocompatibility of the Col I–PLGA films was further tested in primary rabbit corneal endothelial cells (rCEnCs) as models. Compared with bare PLGA films, the Col I–PLGA films displayed the requisite surface roughness, with higher Ra (nm) values, transparency, good hydrophilicity, stability and water uptake. Next, cultured rCEnCs on Col I–PLGA films showed the characteristic polygonal shape of rCEnCs with enhanced initial attachment, proliferation and expression of mRNAs. Collectively, these results indicate that Col I–PLGA can be employed as a suitable alternative for high-quality corneal tissue expansion and transplantation.

Received 12 July 2015; Revised 2 November 2015; Accepted 22 December 2015

Keywords **collagen type I; PLGA; corneal endothelial cells; regeneration; tissue engineering**

1. Introduction

Blindness resulting from corneal disorders/diseases is immensely affecting millions of individuals worldwide, and keratoplasty is the recent standard 'gold therapy' for treating cornea-related issues (Choi *et al.*, 2010; Terry and Ousley, 2006; Gorovoy, 2006; Kageyama *et al.*, 2015). However, the worldwide demand for healthy donor corneas is greatly exceeding the present supply, the scenario becoming worse in an ageing society and with an increased number of young people undergoing corneal laser surgery (Hong *et al.*, 2009). In addition, it is already reported that > 30% human corneal endothelial cells (hCEnCs) are lost within the initial 6 months after surgery (Tan *et al.*, 2012; Price *et al.*, 2010). Therefore, tissue-engineering strategies have been adopted to develop various biological grafts/scaffolds/films as an alternative promising approach for cornea restoration or replacement. A rational graft design for hCEnCs transplantation should have the following features: (a) transparency, water and nutrients permeability, non-cytotoxicity, biodegradability and appropriate mechanical properties; (b) importantly, it should be highly durable for clinically feasible handling and transplantation procedures; and (c) it should support hCEnCs attachment, proliferation, function and survival and be easily integrated into the respective environment. Moreover, the surface characteristics of biological grafts define the specific interface for cell interactions through chemical composition, topography and charge characteristics, and protein adsorption (Chung and Park, 2007; Shah *et al.*, 2011; Yoo *et al.*, 2005). It is well stated that cell adherence is a prerequisite for proper cell and tissue functionality (Giancotti and Ruoslahti, 1999), hence cell attachment ligands bound to graft surfaces, e.g. the

*Correspondence to: G. Khang, Department of BIN Fusion Technology, Department of Polymer Nanoscience and Polymer BIN Research Centre, Chonbuk National University, 567 Baekje-daero, Deokjin-gu, Jeonju 561-756, Republic of Korea. E-mail: gskhang@jbnu.ac.kr
†These authors contributed equally to this study.

integrin-binding tripeptide RGD, can be employed for enhanced cell adherence and spreading (Stevens and George, 2005).

To date, several biodegradable natural and synthetic polymers have been intensively studied for various clinical/biomedical applications. Specifically for regeneration of cornea endothelial cells, several potential biomaterials have been designed, including collagen (Levis *et al.*, 2012), gelatin (Watanabe *et al.*, 2011; Lai *et al.*, 2013), chitosan (Liang *et al.*, 2011; Wang *et al.*, 2012), silk fibroin (Madden *et al.*, 2011; Kim *et al.*, 2015) and decellularized corneal stroma (Choi *et al.*, 2010), etc. Among these, PLGA (a synthetic polymer) and collagen (a natural polymer) have received huge attention for regenerative medicine and tissue-engineering applications. PLGA is a FDA-approved biomaterial for specific clinical applications, including the fabrication of surgical sutures and implantable devices, and mechanically robust, biocompatible and controlled biodegradation in order to match the rate of regeneration of new cells (Munirah *et al.*, 2008; Zhang *et al.*, 2012; Chen, *et al.*, 2000). The roadblocks to these synthetic polymers are lack of cell-recognition signals, resulting in insufficient cell adhesion and hydrophobicity, very little intrinsic surface roughness and limited porosity, owing to the tightly packed, amorphous nature of PLGA (Chen *et al.*, 2000; Forciniti *et al.*, 2010; Mouthuy *et al.*, 2013). On the other hand, in mammalian extracellular matrix, collagen type I (Col I) acts as a potential structural and adhesion protein, facilitating initial cell adherence. It promotes spreading and proliferation via multiple binding sites, including RGD integrin binding sites, being a signalling protein (Sell *et al.*, 2009). Furthermore, the improved biocompatibility of Col I hybridized with several polymers has been widely studied, while the desired mechanical strength of the polymers has been retained (Liu *et al.*, 2008; He *et al.*, 2005; Hokugo *et al.*, 2006; Hartmann-Fritsch *et al.*, 2012). Thus, modification of mechanically strong PLGA with mechanically weak collagen can effectively render the synergetic advantages of both natural and synthetic polymers. In particular, Lu *et al.* (2012) have developed bone morphogenetic protein-4 spatially immobilized in a collagen–PLGA hybrid scaffold, as a promising strategy for bone tissue engineering and bone substitutes. Similarly, Chen *et al.* (2005) fabricated thin PLGA–collagen hybrid mesh and studied this for its possible application for skin tissue engineering.

Despite these advances, a very few studies have been reported regarding the usage of hybrid grafts for cornea tissue engineering. In this study we have fabricated Col I-coated PLGA (Col I–PLGA) film as a potential substrate for the regeneration of corneal endothelial cells. Furthermore, the potency of these Col I–PLGA films was assessed by evaluating the morphology, initial attachment and proliferation capacity, mRNAs expression and histological analysis in rabbit corneal endothelial cells (rCEnCs, used as models).

2. Materials and methods

2.1. Materials

Poly(lactic-co-glycolic acid) (PLGA; MW 90 kDa, lactide: glycolide = 75:25, Resomor® RG755) were purchased from Boehringer Ingelheim Pharma KG (Ingelheim, Germany). Tissue-culture polystyrene (TCP) was purchased from Falcon® (USA). 1,1,1,3,3,3-Hexafluoro-2-propanol (HFIP), acetic acid, phosphate-buffered saline (PBS), collagenase A, glutaraldehyde, dimethyl sulphoxide (DMSO), 3-(4,5-dimethylthiazol-2-yl)-2,5-diphenyl-tetrazolium bromide (MTT), ethidium bromide, $CaCl_2$ and LiBr were purchased from Sigma-Aldrich (St. Louis, MO, USA). Human Col I was obtained from BD Biosciences (USA). Fetal bovine serum (FBS) and 1% penicillin–streptomycin (PS) were purchased from Gibco (USA). 4′,6-Diamidino-2-phenylindole dihydro chloride (DAPI) was obtained from Santa Cruz Biotechnology (USA). Dialysis tube (SnakeSkin® Dialysis Tubing 3,500 MWCO) was purchased from Thermo Science (USA) and used for *in vitro* experiments.

2.2. Fabrication of PLGA and Col I–PLGA film

PLGA films were fabricated by dissolving 5 w/v% PLGA in dichloromethane and then casting into a glass dish, followed by air drying. The film was sterilized by immersion in 70% ethanol and 1× PBS washing. The as-fabricated PLGA film was then coated with human Col I, according to the manufacturer's protocol (BD Biosciences). Briefly, the PLGA film was coated with human Col I (diluted in 0.02 N acetic acid to 5 $\mu g/cm^2$ concentrations under normal air condition without UV) at room temperature for 1 h under UV. The coating solutions were then aspirated to remove remaining acid after 1 h and washed with 1× PBS several times prior to cell seeding.

2.3. Characterizations

The surface morphologies of PLGA and Col I–PLGA films were observed using field emission scanning electron microscopy (FE–SEM; SN-SUPRA 40VP, Carl Zeiss, Germany) and atomic force microscopy (AFM; Multimode-8, Bruker, USA). The transparencies of PLGA and Col I–PLGA films were studied by spectrum analysis, using a Synergy MX spectrophotometer (BioTek®, USA) at a wavelength range of 380–780 nm.

2.4. Contact angle

The hydrophilicity of TCP, PLGA and Col I–PLGA films was measured by analysing the water droplet angle formed between liquid and solid interfaces on the films, using a water contact goniometer (Tantec™, CAM-PLUS Micro, USA).

DOI: 10.1002/term

2.5. Water uptake profile

The water uptake profiles of PLGA and Col I–PLGA films were evaluated by immersing the films in distilled water (DW) for 24 h at 37°C, followed by gentle blot-drying using tissue paper, and then weighed. The wet films were completely dried by lyophilization and again reweighed. Total water uptake (*WU*) of the films was calculated according to the following equation (Liu *et al.*, 2008):

$$WU\,(\%) = \left(W_{\text{wet}} - W_{\text{dry}}\right)/W_{\text{wet}} \times 100$$

where W_{wet} and W_{dry} are the wet weight and the dry weight of films at each time point, respectively.

2.6. *In vitro* biodegradability

First the PLGA, Col I–PLGA films were cut into small pieces (~1 cm in diameter) and the initial dried weight of the samples was measured. These cut pieces were then incubated in 1 U/ml collagenase A in 9.57 mM PBS, pH 7.35–7.65, for 21 days at 37°C. Next, each sample was weighed at different time intervals and the residual mass (*RM*) was calculated using the following equation (Liu *et al.*, 2008):

$$RM\,(\%) = W_{\text{t}}/W_{\text{i}}$$

where W_{i} and W_{t} are the initial weight and the weight of the sample measured at each time point, respectively.

2.7. Isolation and culture of rCEnCs

To obtain rCEnCs, eyeballs were extracted from New Zealand White rabbits, aged 4 weeks. After the cornea was cut from the eyeball, Descemet's membrane containing endothelium was peeled from the stroma under a stereoscopic microscope and digested in collagenase A for 40 min at 37°C. After the incubation of rCEnCs, culture medium was added to stop the digestion process, followed by its collection through centrifugation. Then the isolated primary rCEnCs were plated in endothelial growth medium-2 (EGM-2, Lonza, Walkersville, MD, USA) containing 10% FBS and 1% PS. The culture medium was changed every other day.

2.8. Morphology, initial attachment and proliferation assay

First, rCEnCs were cultured on TCP, PLGA and Col I–PLGA films at a density of 100 cells/mm^2. After reaching cell confluence, the culture medium was replaced with fresh medium and the cell morphology was observed using light microscopy (Nikon Eclipse TE2000U, Nikon, Japan). Then SEM analysis was performed after treating the cell samples with 2.5% scanning electron microscopy (SEM)-grade glutaraldehyde (diluted in 1× PBS) for 24 h at room temperature, followed by drying of the samples using a critical point dryer (EMS 850, Electron Microscopy Sciences, Hatfield, PA, USA), and finally the images were obtained by FE–SEM (SN-SUPRA 40VP, Carl Zeiss, Germany).

In order to check the initial density, rCEnCs (2000 cells/mm^2 density) were seeded on TCP, PLGA and Col I–PLGA films and cultured in endothelial basal medium (EBM; Lonza, Walkersville, MD, USA) for 20 min. After completion of the incubation time, the samples were fixed with 10% neutral formalin for 20 min at room temperature and stained with DAPI. All the images were obtained using a fluorescence microscope and the nuclear number (cells/mm^2) was counted using the ImageJ program ($n = 5$).

rCEnCs proliferation was assessed using the MTT assay. In brief, rCEnCs were seeded (100 cells/mm^2/well) on TCP, PLGA and Col I–PLGA films and cultured in EGM-2 for 1, 3 and 5 days. At each time point, the samples were washed with 1× PBS, followed by the addition of MTT solution (50 mg/ml in PBS) in fresh culture medium (10% MTT of medium volume) and incubated for 4 h at 37°C and 5% CO_2. Then the solution was aspirated, 1 ml DMSO was added to solubilize the formazan crystals and the mixture kept for 30 min at 4°C. Finally, the reaction product absorbance was analysed at 570 nm, using a microplate reader (Synergy MX, Biotek, USA). All the experiments were performed in triplicate.

2.9. Evaluation of mRNAs expression

Total RNA was extracted from cultured passage 1 rCEnCs on TCP, PLGA and Col I–PLGA films, using TRIzol reagent (Takara, Japan) according to the manufacturer's instructions, and the samples were quantified using an Eppendorf BioSpectrometer® (Eppendorf, Germany). The gene markers were amplified as follows: β-actin, aquaporin-1, collagen type VIII, Na^+/K^+-ATPase, chloride channel protein 3 (CLCN3), sodium/bicarbonate cotransporter (NBC1), voltage-dependent anion-selective channel 2 (VDAC2) and voltage-dependent anion-selective channel 3 (VDAC3), to confirm the interactions between Col I and rCEnCs. First, the samples were denatured for 30 s at 95°C, followed by 30 s annealing at the primer-specific temperature and 1 min/kb elongation at 72°C. The gene primer for rCEnCs was designed according to previously reported literature (Kim *et al.*, 2015). Then the polymerization chain reaction (PCR) products were separated by electrophoresis at 100 V on 1.0% agarose gel in 0.5% TAE (Tris-acetate-EDTA) buffer and visualized using ethidium bromide staining.

2.10. Histological analysis

The rCEnCs identity was confirmed by monitoring the expressions of Na^+/K^+-ATPase and ZO-1. In brief, the cell-seeded films were fixed with 10% neutral formalin for 20 min at room temperature and incubated with anti-

DOI: 10.1002/term

Na^+/K^+-ATPase and anti-ZO-1 (1:150; Santa Cruz Biotechnology) as primary antibodies. Fluorescein-labelled goat anti-mouse IgG (1:300; Santa Cruz Biotechnology) and AlexaFluor® 594-conjugated AffiniPure donkey anti-rabbit IgG (1:300; Jackson Immuno Research Laboratories, USA) as secondary antibodies were used for the detection of Na^+/K^+-ATPase and ZO-1. Finally images were taken using a confocal laser-scanning microscope (LSM 510 META, Carl Zeiss, Germany).

2.11. Statistical analysis

Each experiment was performed in triplicate. Data are presented as mean ± standard deviation (SD). Statistical analysis was conducted based on Student's *t*-test (Excel 2007, Microsoft) and the differences were considered significant at $*p < 0.05$, $**p < 0.01$ and $***p < 0.001$.

3. Results and discussion

3.1. Surface morphology

The surface characteristics of the designed construct, such as surface topology (roughness), wettability, surface energy, surface charge and stiffness, greatly affect the biological functions of cells, including cell adhesion, spreading, proliferation, growth patterns and so on. Figure 1 displays the topology and roughness of bare PLGA and Col I–PLGA film analysed by FE–SEM and three-dimensional (3D) AFM images. FE–SEM images of bare PLGA film (Figure a1) exhibit a smooth surface prior to surface functionalization; however, the Col I–PLGA film (Figure b1) demonstrates rough and irregular surface morphology with pore-like structures on the films. Furthermore, a detailed analysis of morphology and roughness/smoothness of the films was performed using AFM images. Presenting an excellent consistency with the FE–SEM images, the AFM images of bare PLGA (Figures a2, 3) show regular and smoothed surface morphology, whereas the Col I–PLGA films (Figures b2, 3) show an irregular and rugged surface morphology. Compared to bare PLGA [root mean square roughness (R_{rms}) = ~1.36 nm], a low R_{rms} value of ~ 2.07 nm is observed for Col I–PLGA film. These preliminary results suggest that surface functionalization of PLGA with Col I can enhance the surface properties, which may facilitate initial cellular adhesion and proliferation, essential for the regeneration of corneal endothelial cells.

3.2. Transparency

Optical transparency of the designed biological construct is highly crucial for corneal endothelium transplantation, since acellular human cornea stroma is reported to exhibit ~88–90% transmittance at a wavelength of 400–650 nm and > 90% only at the 'far red' (Chung and Park, 2007). Figure 2a depicts the transparency profile of TCP, PLGA and Col I–PLGA films in the visible range, along with their comparative optical images (inset). As a positive control, TCP demonstrates the highest transparency when observed both with and without cells. The optical transmittance results show that both PLGA and Col I–PLGA films are highly transparent, consistent with the optical images.

3.3. Surface hydrophilicity/hydrophobicity

Surface hydrophilicity/hydrophobicity of the designed construct is highly crucial for initial cellular adhesion and further growth (Kobayashi *et al.*, 2014). In order to know the potency of Col I–PLGA films for cell adherence and proliferation, the surface hydrophilicity/hydrophobicity for the films were assessed by measuring the contact angle of a

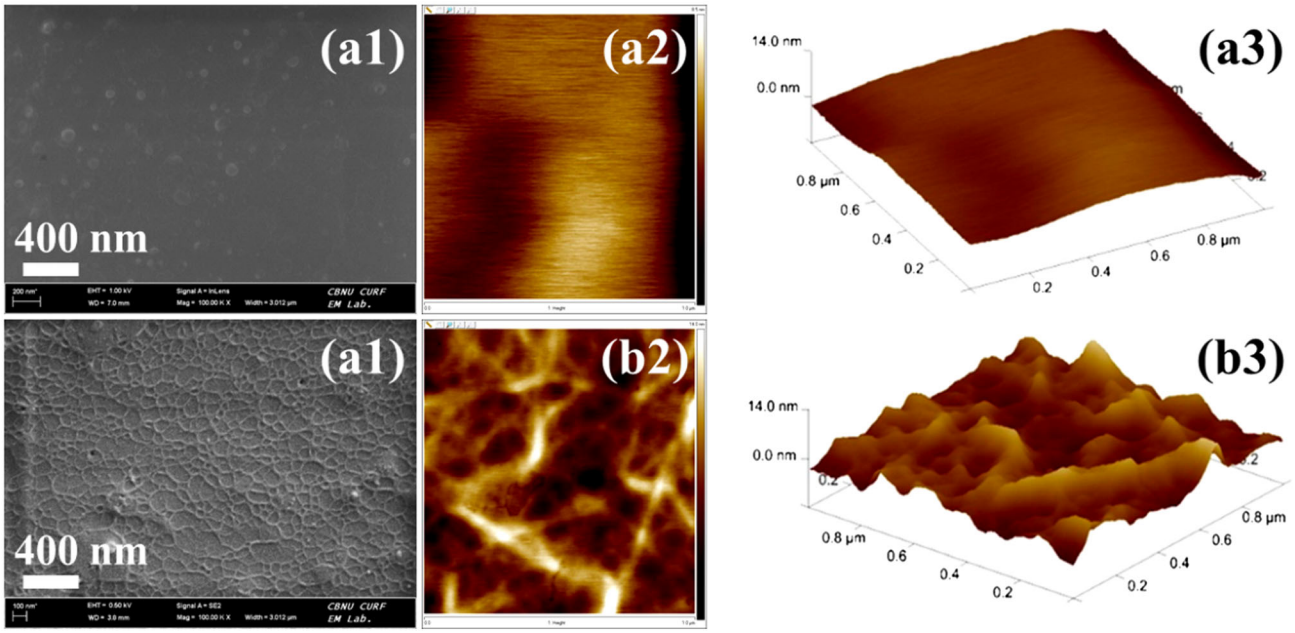

Figures 1. (a1) FE–SEM and (a2, 3) AFM images of PLGA film. (b1) FE–SEM and (b2, 3) AFM images of as-fabricated Col I–PLGA film

DOI: 10.1002/term

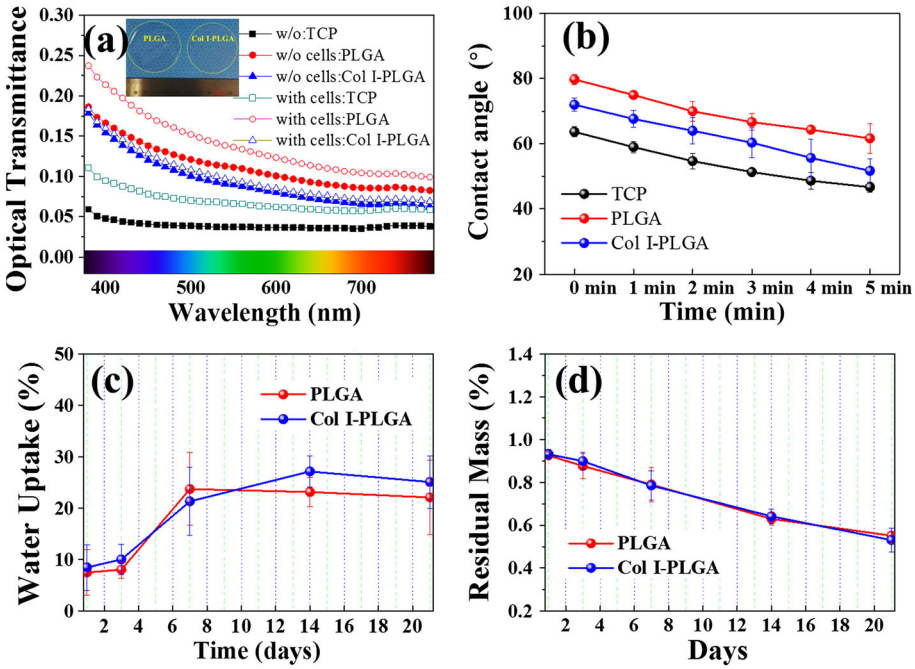

Figure 2. (a) Transparency results of the TCP, PLGA and Col I–PLGA films in the visible wavelength range 380–780 nm; (inset) comparative optical images of PLGA and Col I/ PLGA films. (b) Surface hydrophilicity/hydrophobicity analysis of the TCP, PLGA and Col I–PLGA films by measuring the contact angle of a single water droplet on the films, observed for 5 min; *$p < 0.5$. (c) Water uptake behaviour. (d) *In vitro* degradation

single water droplet on the films at different time intervals, as shown in Figure 2b. A reduction in contact angle of the single water droplet on the films indicates an increase in the hydrophilicity of the construct. Depending on the obtained contact angle results, the hydrophilicity of the films can be ranked in the order: PLGA < Col I–PLGA < TCP. This suggests that the Col I–PLGA films can provide a friendly environment for cellular adhesion and proliferation.

3.4. Water uptake and *in vitro* degradation analysis

One of the major functions of the corneal endothelium is maintaining proper water uptake and oedema of the corneal stroma. Thus, the fabricated environment must support a cultured corneal endothelium function having proper water uptake properties (Edelhauser, 2006). Figure 2c shows the water uptake profile of PLGA and Col I–PLGA films. Both the films showed a gradual increase in the water uptake profile and reached a plateau on day 14. Compared with the PLGA films (~22%), the Col I–PLGA films (~26%) showed a slight increase in water uptake behaviour (day 14). On day 20, we observed nearly negligible reduction in water uptake capacity for PLGA and Col I–PLGA films, suggesting good stability of the films. Moreover, Figure 2d shows the *in vitro* biodegradation of PLGA and Col I–PLGA films. Until day 6, a rapid decrement in the residual mass was evident, followed by a slow decrease up to day 20. Almost similar results were obtained for both the films, which further suggests the absence of any remarkable effects on the water uptake and *in vitro* degradation profile of the Col I–PLGA films owing to the Col I coating.

3.5. *In vitro* biological performance

3.5.1. *Cell adhesion, migration and proliferation*

Initial cell adhesion onto the bioengineered construct surface is considered to be the first vital step for creating cell function-regulating materials. The cells' structural organization over the construct surface also plays an important deciding parameter regarding the degree and direction of cell movement and growth upon it (Smith *et al.*, 2004; Braam *et al.*, 2008). A slow adherence of cells onto the construct shows low affinity towards it, and vice versa (Chen *et al.*, 2009). Therefore, a resultant low initial cell attachment rate will require a longer time to reach the required confluence, consequently resulting in a remarkable decrease in the final yield following donor sample preparation and the isolation process. In order to determine the *in vitro* biological potential of the Col I–PLGA films, we studied the initial attachment, morphology and organization of cultured rCEnCs for 1, 3, 5 and 7 days. Figure 3a shows the initial attachment of rCEnCs on TCP, PLGA and Col I–PLGA films 20 min after seeding in serum-free medium at a density of 2000 cells/mm^2. It is well known that the minimum cell density required for maintaining functions of corneal endothelial cells is about 500 cells/mm^2 (Joyce, 2003). As a positive control, TCP (a commercially available material) showed the highest cell density. The Col I–PLGA films showed an enhanced cell growth and number, i.e. ca. 900 cells/mm^2, compared with bare PLGA films. This can be attributed to

DOI: 10.1002/term

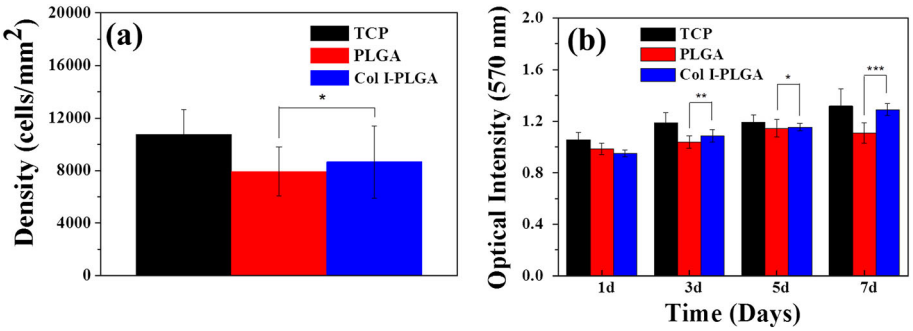

Figure 3. *In vitro* **rCEnCs behavioural study. (a) Initial attachment of rCEnCs after 20 min seeding in serum-free medium; and (b) proliferation assay by MTT in EGM-2. Each experiment was performed in triplicate; *$p < 0.05$, **$p < 0.01$, ***$p < 0.001$**

the surface coating of PLGA with Col I, consisting of an RGD sequence required for the recognition for integrin-mediated cell adhesion and growth (Sell *et al.*, 2009).

Next, the cytocompatibility of all the films was analysed using the MTT proliferation assay, as shown in Figure 3b. Overall, all films demonstrated time-dependent cellular growth. As compared with bare PLGA films, the Col I–PLGA films displayed a significant increment in cell viability, especially on days 3, 5 and 7. These results further indicate that Col I–PLGA films can serve as a promising platform for rCEnCs carriers because of the adhesive properties of Col I.

3.5.2. Cellular monolayer formation and phenotype maintenance

Figure 3c, d, shows comprehensive analysis of the cultured rCEnCs morphology and phenotype on the films, performed using light microscopy and FE–SEM after 5 days of cells culture. After day 1 in culture, a greater initial rCEnCs adherence onto the Col I–PLGA films was found, with the cells showing a characteristic polygonal shape; however, the rCEnCs reached confluence on day 3 (data not shown). On day 5 of culture, the images showed well-grown, well-maintained rCEnCs

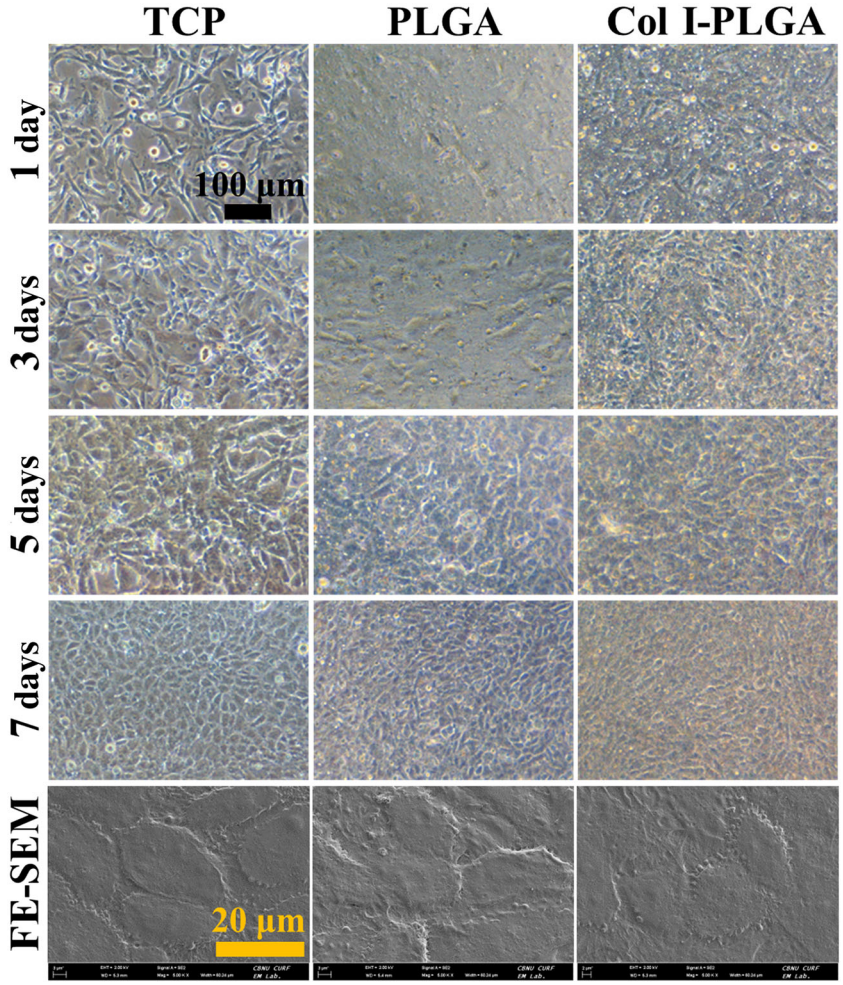

Figure 4. Light microscopic and FE–SEM images of cell morphology after 5 days of culture

DOI: 10.1002/term

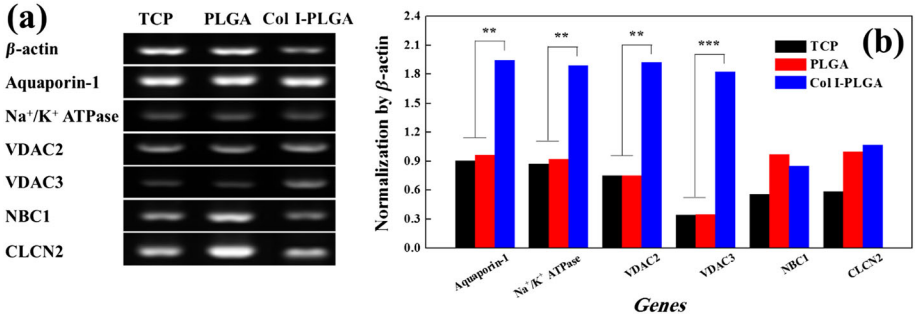

Figure 5. mRNA expression of rCEnCs. (a) Electrophoresis assay using specific cell markers. (b) Normalization by β-actin. Each experiment was performed in triplicate; $^{**}p < 0.01$, $^{***}p < 0.001$

on the Col I–PLGA films compared with the bare PLGA films. Soon after this cultivation time, all the films demonstrated rCEnCs monolayer formation. However, we observed a faster formation of rCEnCs monolayer on Col I–PLGA films, which can be ascribed to the Col I functionalization acting, as the structural/adhesion protein resulting in enhanced cellular adherence, migration and proliferation.

3.5.3. Expressions of specific mRNAs and functional protein

The expressions of specific mRNAs associated with rCEnCs were studied on TCP, PLGA and Col I–PLGA films by evaluating diverse genes, such as Aquaporin-1 (*AQ*), Na^+/K^+-ATPase (*NaK*), voltage-dependent anion channel 2 (*VDAC2*), voltage-dependent anion channel 3 (*VDAC3*), Na^+-HCO co-transporter (*NBC1*) and chloride channel protein 2 (*CLCN2*), using RT–PCR. *AQ* serves a vital role in fluid transport and *NaK* has an effect on the transparency and permeability of the cornea through pump function (Verkman, 2002). *VDAC2* and *VDAC3* control the interaction of proteins and small molecules between adjacent cells (Yee *et al.*, 1985). *CLCN3* has a crucial role on physiological phenomena, such as controlling pH, transporting organic molecules, cellular migration, differentiation and proliferation (Sampson *et al.*, 1996). Figure 4a displays the results of gene expressions obtained by electrophoresis from amplified genes and Figure 4b shows the normalization results by β-actin. We observed good expression of genes for bare PLGA films and TCP. Compared with PLGA films and TCP, the cultured rCEnCs on Col I–PLGA films showed significant enhancement in expressions of AQ, NaK, VDAC2 and VDAC3. However, a slight increase in CLCN2 expression and little decrease in NBC1 expression were also noticed for Col I–PLGA films. This implied that the Col I–PLGA films render a friendly environment for cell–cell interaction, cellular growth and expression of genes. Figure 5 and 6 shows the expression of NaK (sodium potassium pump amenable for controlling water from the corneal stroma) and ZO-1 (tight junction protein zona ocludin-1) on TCP, PLGA and Col I–PLGA films. The images showed that the rCEnCs have well-expressed NaK and ZO-1 on all the films, along with well-maintained cell morphology.

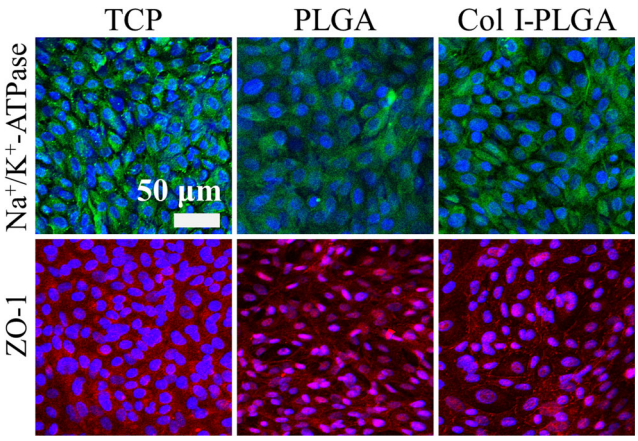

Figure 6. Immunofluorescence microscopy of rCEnCs. (a) Na^+/K^+-ATPase. (b) Zona occludens-1 (ZO-1)

Further, these results indicate that Col I–PLGA films can be envisioned as a potential rCEnCs carrier with the desired biofunctionality for future corneal transplantation applications.

4. Conclusion

We have designed a highly-compatible, transparent, biodegradable Col I–PLGA film in order to incorporate specific functionality for enhanced rCEnCs adhesion, migration and proliferation, whilst limiting the probability of non-specific interactions between the construct and the biological environment. *In vitro* results showed that the Col I–PLGA film efficiently increases the initial rCEnCs adherence, maintains cellular migration, growth, cell phenotype, formation of cell junctions and gene expression required for functional rCEnCs. Thus, this bioengineered construct containing an expandable population of rCEnCs could be further used to address the present issue of shortage of corneas required for corneal repair procedures.

Conflict of interest

The authors have declared that there is no conflict of interest.

DOI: 10.1002/term

Acknowledgements

This research was supported by the Bio & Medical Technology Development Programme of the National Research Foundation of Korea (NRF), funded by the Korean government (MEST; Grant No. NRF-2012M3A9C60 50204), and BK21 PLUS.

References

Braam S, Zeinstra L, Litjens S *et al.* 2008; Recombinant vitronectin is a functionally defined substrate that supports human embryonic stem cell self-renewal via $\alpha V\beta 5$ integrin. *Stem Cells* **26**: 2257–2265.

Chen G, Ushida T, Tateishi T *et al.* 2000; Hybrid biomaterials for tissue engineering: a preparative method for PLA or PLGA–collagen hybrid sponges. *Adv Mater* **12**: 455–457.

Chen G, Sato T, Ohgushi H *et al.* 2005; Culturing of skin fibroblasts in a thin PLGA–collagen hybrid mesh. *Biomaterials* **26**: 2559–2566.

Chen M, Patra PK, Lovett ML *et al.* 2009; Role of electrospun fibre diameter and corresponding specific surface area (SSA) on cell attachment. *J Tissue Eng Regen Med* **3**: 269–279.

Choi JS, Williams JK, Greven M *et al.* 2010; Bioengineering endothelialized neocorneas using donor-derived corneal endothelial cells and decellularized corneal stroma. *Biomaterials* **31**: 6738–6745.

Chung HJ, Park TJ. 2007; Surface engineered and drug releasing prefabricated scaffolds for tissue engineering. *Adv Drug Deliv Rev* **59**: 249–262.

Edelhauser HF. 2006; The balance between corneal transparency and edema – the Proctor lecture. *Invest Ophthalmol Vis Sci* **47**: 1755–1767.

Forciniti L, Guimard NK, Lee S *et al.* 2010; Unique electrochemically synthesized polypyrrole:poly(lactic-co-glycolic acid) blends for biomedical applications. *J Mater Chem* **20**: 8865–8874.

Giancotti FG, Ruoslahti E. 1999; Integrin signaling. *Science* **285**: 1028–1033.

Gorovoy MS. 2006; Descemet-stripping automated endothelial keratoplasty. *Cornea* **25**: 886–889.

Hartmann-Fritsch F, Biedermann T, Braziulis E *et al.* 2012; Collagen hydrogels strengthened by biodegradable meshes are a basis for dermo-epidermal skin grafts intended to reconstitute human skin in a one-step surgical intervention. *J Tissue Eng Regen Med* **10**: 81–91.

He W, Yong T, Teo WE *et al.* 2005; Fabrication and endothelialization of collagen-blended biodegradable polymer nanofibers: potential vascular graft for blood vessel tissue engineering. *Tissue Eng* **11**: 1574–1588.

Hokugo A, Takamoto T, Tabata Y *et al.* 2006; Preparation of hybrid scaffold from fibrin and biodegradable polymer fiber. *Biomaterials* **27**: 61–67.

Hong J, Xu J, Sun X *et al.* 2009; Tissue-engineered corneal stroma by using autologous adipose derived stem cell tissue and polylactic cocglycolic acid. World Congress on Medical Physics and Biomedical Engineering. *IFMBE Proc* **25**: 1–5.

Joyce NC. 2003; Proliferative capacity of the corneal endothelium. *Prog Retin Eye Res* **22**: 359–389.

Kageyama T, Hayashi R, Hara S *et al.* 2015; Spontaneous acquisition of infinite proliferative capacity by a rabbit corneal endothelial cell line with maintenance of phenotypic and physiological characteristics. *J Tissue Eng Regen Med*. DOI:10.1002/term.2005.

Kim EY, Tripathy N, Park JY *et al.* 2015; Silk fibroin film as an efficient carrier for corneal endothelial cells regeneration. *Macromol Res* **23**: 189–195.

Kobayashi Y, Hirose M, Sogo Y *et al.* 2014; Study on the correlation between initial attachment morphology and osteogenic differentiation of rat mesenchymal stems cells under controlling their metabolism. *Int J Tissue Regen* **5**: 9–13.

Lai JY, Ma DHK, Lai MH *et al.* 2013; Characterization of cross-linked porous gelatin carriers and their interaction with corneal endothelium: biopolymer concentration effect. *PLoS ONE* **8**: e54058.

Levis HJ, Peh GSL, Toh KP *et al.* 2012; Plastic compressed collagen as a novel carrier for expanded human corneal endothelial cells for transplantation. *PLoS ONE* **33**: 50993.

Liang Y, Liu W, Han B *et al.* 2011; Fabrication and characters of a corneal endothelial cells scaffold based on chitosan. *J Mater Sci Mater Med* **22**: 175–183.

Liu W, Merrett K, Griffith M *et al.* 2008; Recombinant human collagen for tissue engineered corneal substitutes. *Biomaterials* **29**: 1147–1158.

Lu H, Kawazoe N, Kitajima T *et al.* 2012; Spatial immobilization of bone morphogenetic protein-4 in a collagen–PLGA hybrid scaffold for enhanced osteoinductivity. *Biomaterials* **33**: 6140–6146.

Madden PW, Lai JN, George KA, Giovenco T, Harkin DG, Chirila TV 2011; Human corneal endothelial cell growth on a silk fibroin membrane. *Biomaterials* **32**: 4076–4084.

Mouthuy PA, El-Sherbini Y, Cui Z *et al.* 2013; Layering PLGA-based electrospun membranes and cell sheets for engineering cartilage–bone transition. *J Tissue Eng Regen Med*. DOI:10.1002/term.1765.

Munirah S, Kim SH, Ruszymah BH *et al.* 2008; The use of fibrin and poly(lactic-co-glycolic acid) hybrid scaffold for articular cartilage tissue engineering: an *in vivo* analysis. *Eur Cells Mater* **15**: 41–52.

Price MO, Gorovoy M, Benetz BA *et al.* 2010; Descemet's stripping automated endothelial keratoplasty outcomes compared with penetrating keratoplasty from the Cornea Donor Study. *Ophthalmology* **117**: 438–444.

Sampson MJ, Lovell RS, Davison DB *et al.* 1996; A novel mouse mitochondrial voltage-dependent anion channel gene localizes to chromosome 8. *Genomics* **36**: 192–196.

Sell SA, McClure MJ, Garg K *et al.* 2009; Electrospinning of collagen/biopolymers for regenerative medicine and cardiovascular tissue engineering. *Adv Drug Deliv Rev* **61**: 1007–1019.

Shah A, Shah S, Mani G *et al.* 2011; Endothelial cell behaviour on gas-plasma-treated PLA surfaces: the roles of surface chemistry and roughness. *J Tissue Eng Regen Med* **5**: 301–312.

Smith CM, Stone AL, Parkhill RL *et al.* 2004; Three-dimensional bioassembly tool for generating viable tissue-engineered constructs. *Tissue Eng* **10**: 1566–1576.

Stevens MM, George JH. 2005; Exploring and engineering the cell surface interface. *Science* **310**: 1135–1138.

Tan DT, Dart JK, Holland EJ *et al.* 2012; Corneal transplantation. *Lancet* **379**: 1749–1761.

Terry MA, Ousley PJ. 2006; Deep lamellar endothelial keratoplasty: early complications and their management. *Cornea* **25**: 37–43.

Verkman AS. 2002; Aquaporin water channels and endothelial cell function. *J Anat* **200**: 617–627.

Wang TJ, Wang IJ, Lu JN *et al.* 2012; Novel chitosan–polycaprolactone blends as potential scaffold and carrier for corneal endothelial transplantation. *Mol Vis* **18**: 255–264.

Watanabe R, Hayashi R, Kimura Y *et al.* 2011; A novel gelatin hydrogel carrier sheet for corneal endothelial transplantation. *Tissue Eng A* **17**: 2213–2219.

Yee RW, Geroski DH, Matsuda M *et al.* 1985; Correlation of corneal endothelial pump site density, barrier function, and morphology in wound repair. *Invest Ophthalmol Vis Sci* **26**: 1191–1201.

Yoo HS, Lee EA, Yoon JJ *et al.* 2005; Hyaluronic acid modified biodegradable scaffolds for cartilage tissue engineering. *Biomaterials* **26**: 1925–1933.

Zhang Y, Yang F, Liu K *et al.* 2012; The impact of PLGA scaffold orientation on *in vitro* cartilage regeneration. *Biomaterials* **33**: 2926–2935.